

## Neutron-Diffraction Study of $\text{UO}_2$ : Observation of an Internal Distortion\*

J. Faber, Jr., and G. H. Lander  
Argonne National Laboratory, Argonne, Illinois 60439

and

B. R. Cooper  
Department of Physics, West Virginia University, Morgantown, West Virginia 26506  
(Received 3 November 1975)

We have deduced from measurements of the neutron elastic cross section that below the Néel temperature ( $T_N$ ) the oxygen atoms in  $\text{UO}_2$  are shifted from their ideal fluorite positions. We find quantitative agreement with experiment by assuming a rearrangement (internal shear deformation with amplitude 0.014 Å) of the oxygen sublattice. The dominance of this deformation mode in the spin-lattice interactions suggests the presence of a non-collinear magnetic structure in  $\text{UO}_2$ .

The antiferromagnetic structure and the first-order paramagnetic-to-antiferromagnetic phase transition in  $\text{UO}_2$  (fluorite crystal structure) were first reported by Frazer *et al.*<sup>1</sup> Following detailed measurements of the spin-wave spectra,<sup>2</sup> elastic constants,<sup>3</sup> and infrared spectra,<sup>4</sup> Allen<sup>4,5</sup> proposed a microscopic theory to explain the first-order transition in terms of a cooperative Jahn-Teller effect. A novel feature of this theory is the prediction that an internal strain is the dominant distortion mode for the spin-lattice coupling without the requirement of a significant macroscopic distortion. No observation of such an effect has been reported. In this Letter, we present the results of neutron elastic-scattering measurements for  $\text{UO}_2$  in the ordered state. The experiments show that the oxygen atoms are displaced from their ideal fluorite positions below  $T_N$ . The resultant distortion is an internal shear deformation, and we recognize that this deformation dominates the magnetic behavior of  $\text{UO}_2$  through strong spin-lattice coupling.<sup>2</sup>

The magnetic structure of  $\text{UO}_2$  is type I, which consists of ferromagnetic (001) planes stacked in an alternating + - sequence.<sup>1</sup> In a multidomain sample, the precise direction of the magnetic moment cannot be determined, but it does lie in the (001) plane. The magnetic reciprocal-lattice points, which have mixed indices such that  $h+k$  = even, and  $h+l$  = odd, are completely separate from the nuclear reciprocal-lattice points. The intensities of 1250 magnetic reflections (reducing to 71 inequivalent  $hkl$  values) from a well-characterized single crystal (1.6 by 2.4 by 5.1 mm<sup>3</sup>) of  $\text{UO}_2$  at 4.2 K have been measured<sup>6</sup> with the cryo-orienter assembly at the CP-5 research reactor. The magnetic intensities may be re-

duced to  $\mu f(\vec{\kappa})$  values by

$$I_M = 72.7(C/3)[\mu f(\vec{\kappa})]^2 \exp(-2W_U)q^2 A y / \sin 2\theta \quad (1)$$

mb/mole,

where  $I_M$  is the observed magnetic scattering intensity,  $C$  is the scale factor derived from the nuclear reflections, the factor of  $\frac{1}{3}$  arises from the number of magnetic domains,  $\mu$  is the magnetic moment in Bohr magnetons,  $f(\vec{\kappa})$  is the magnetic form factor,  $\vec{\kappa}$  is the scattering vector,  $W_U = B_U \sin^2 \theta / \lambda^2$  is the Debye-Waller factor for the uranium atoms,  $q^2$  is the square of the magnetic interaction vector,  $y$  is the extinction factor,  $A$  is the absorption factor, and  $2\theta$  is the scattering angle. Small extinction corrections (<5%) were necessary only for the first two magnetic reflections. Under the assumption that the intensities are entirely magnetic in origin, the values of  $\mu f(\vec{\kappa})$  are derived from Eq. (1) and plotted versus  $\sin \theta / \lambda$  in Fig. 1.

The theoretical magnetic cross section  $d\sigma_M$  has been calculated with the tensor-operator method<sup>7</sup> and the Dirac-Fock radial wave functions.<sup>8</sup> The ground state of  $\text{U}^{4+}$  in  $\text{UO}_2$ , with two unpaired  $5f$  electrons, is a  $\Gamma_5$  triplet, arising primarily from the Russell-Saunders, Hund's rule  $^3H_4$  configuration.<sup>9</sup> Full details of these calculations will be published elsewhere; however, the important point here is that the calculated values of  $\mu f(\vec{\kappa})$  all fall between the broken curves in Fig. 1. At low scattering angles, the observed intensities are in agreement with theory and extrapolate to give a magnetic moment of  $(1.74 \pm 0.02)\mu_B$  per U atom at  $\kappa=0$ . For  $|\vec{\kappa}|/4\pi = \sin \theta / \lambda > 0.5 \text{ \AA}^{-1}$ , a number of points lie well above the calculated values. Similar discrepancies were obtained with a limited set of reflections from a second crystal

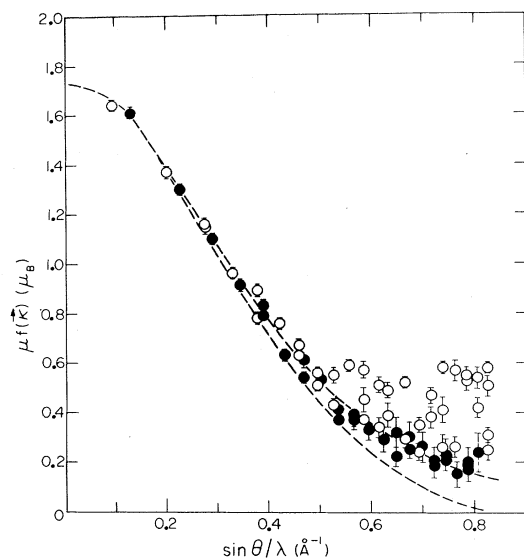


FIG. 1. Experimental values of  $\mu f(\vec{\kappa})$  for  $\text{UO}_2$  at 4.2 K. The open circles are magnetic reflections with  $h$  and  $k$  even and  $l$  odd; the closed circles are reflections with  $h$  and  $k$  odd and  $l$  even. The broken lines enclose an envelope containing the calculated values of  $\mu f(\vec{\kappa})$ .

of  $\text{UO}_2$ .

A careful examination of Fig. 1 shows that for  $\sin \theta/\lambda > 0.5 \text{ \AA}^{-1}$  only a certain subset of reflections (open circles) lies outside the envelope defined by the broken lines. We can represent the behavior of the two subsets more clearly by plotting the difference cross section  $d\sigma_{\text{obs}} - d\sigma_M$  in Fig. 2(a). The solid circles show that for the subset with  $l$  even, theory and experiment are in good agreement, except for a small constant background of  $\sim 0.3 \text{ mb/mole}$ , which probably arises from multiple scattering. In contrast, the subset with  $l$  odd exhibits additional scattering that is not simply dependent on  $\vec{\kappa}$  and is unlikely to be magnetic in origin, since it increases as  $\kappa$  increases. These intensities are  $< 10^{-3}$  of the nuclear Bragg reflections.

Following Allen's theory,<sup>4,5</sup> we anticipate that Jahn-Teller interactions are important in  $\text{UO}_2$  and consider whether the additional scattering in Fig. 2(a) arises from small (static) displacements of the atoms from their equilibrium positions. Allen considered the local distortions of the oxygen sublattice that transform as the representations contained in the symmetric square  $[\Gamma_5^2]$  and obtained the normal modes with  $E_g$  and  $T_{2g}$  symmetry. The two  $E_g$  modes,  $Q_\theta$  and  $Q_\epsilon$ , correspond to tetragonal and orthorhombic deformations, respectively. The  $T_{2g}$  modes are  $Q^1$ ,

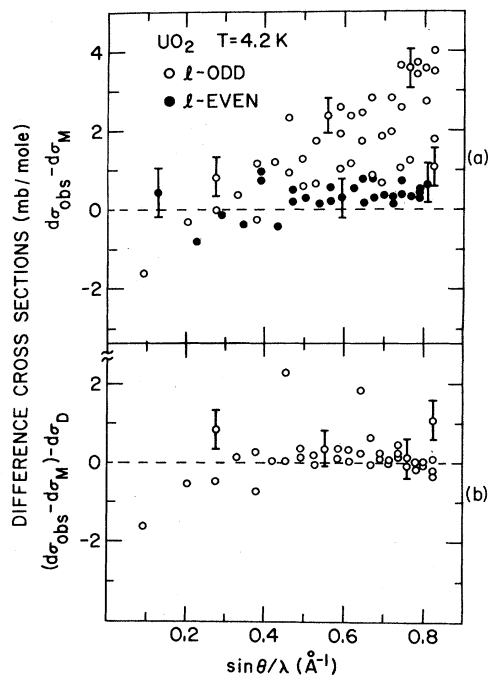


FIG. 2. (a) The theoretical magnetic cross section  $d\sigma_M$  subtracted from each observed intensity  $d\sigma_{\text{obs}}$ . The open and closed circles are as in Fig. 1. (b) Only the  $l$ -odd subset is shown with the internal-distortion cross section  $d\sigma_D$  subtracted.

which corresponds to a shear deformation, and  $Q^2$ , which corresponds to the *internal* distortion discussed by Allen. All these modes are homogeneous deformations (corresponding to  $q=0$  phonons) and, except for the  $Q^2$  modes, which correspond to optic phonons, lead to a reduction in the symmetry of the unit cell. Low-temperature x-ray experiments<sup>10</sup> have failed to detect any change in the overall symmetry of the unit cell, and experiments recently performed at Argonne National Laboratory confirm the previous results.<sup>11</sup> In the context of Allen's model, our results should therefore be compatible with the  $T_{2g}(Q^2)$  mode. Unfortunately this mode, in which the two oxygen tetrahedra move against one another, does not produce intensity at the magnetic reciprocal-lattice points. Instead, the intensities of the fundamental fluorite reflections are modified.

The absence of any appreciable macroscopic distortion and the failure of the  $Q^2$  internal mode to account for the neutron results lead us to consider *inhomogeneous* deformations. Noting the anomalous behavior of the  $C_{44}$  elastic constant,<sup>3</sup> we choose a static configuration based on the  $Q^1$

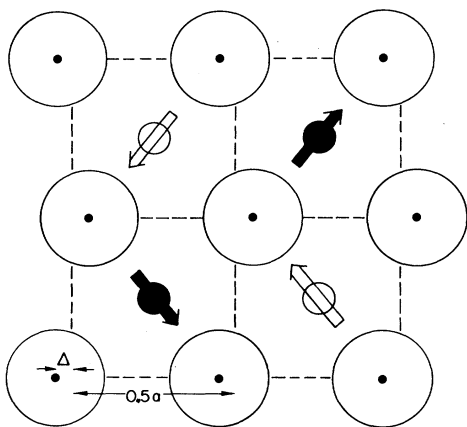


FIG. 3. The (001) projection of the fluorite structure. The closed and open circles represent uranium atoms at  $z=0$  and  $z=\frac{1}{2}$ , respectively. The large circles represent oxygen atoms at  $z=\frac{1}{4}$  and  $z=\frac{3}{4}$  displaced from the ideal fluorite lattice (indicated by the dashed lines). The shift of the oxygen atoms is not drawn to scale,  $\Delta/a=2.6 \times 10^{-3}$ . The suggested noncollinear spin configuration is also shown.

shear deformation, but with the sense of the atomic displacements of nearest-neighbor oxygen atoms rotated by  $\pi$  between adjacent uranium atoms. (One possible model is shown in Fig. 3.) A similar procedure, involving a uniform dilation instead of a rotation, may be followed for the  $E_g$  modes. In all these deformations the uranium sublattice remains undisturbed. To test the various mode configurations, we have performed a least-squares refinement with the quantities  $d\sigma_{\text{obs}} - d\sigma_M$  of Fig. 2(a) as experimental input. The calculated cross section  $d\sigma_D$  arises from the oxygen displacements. The analysis with the deformations based on  $E_g$  modes leads to non-zero  $d\sigma_D$  values at the magnetic reflections but fails to give even qualitative agreement with experimental data ( $\chi^2=21$ ). In contrast, the analysis with the internal shear deformation of Fig. 3 given an excellent fit to experimental data ( $\chi^2=1$ ), as illustrated by plotting the point-by-point residual in Fig. 2(b). The *only* parameter in this fit is  $\Delta$ , the fractional coordinate shift of the oxygen atom from its equilibrium position. As a result of domain averaging,  $\Delta$  is a radial quantity. A least-squares fit gives  $\Delta=(2.6 \pm 0.2) \times 10^{-3}$ , which implies a shift in the oxygen position of  $0.014 \text{ \AA}$ . This deformation does not contribute to the magnetic reflections with  $l$  even.

Considering inhomogeneous deformations, we have introduced additional internal modes, which

are contained in the symmetric square  $[\Gamma_5^2]$ . These modes are constructed by combining  $T_{2g}(Q^1)$  with a pure rotation  $T_{1g}$  and combining  $E_g$  with a uniform dilation  $A_{1g}$ . The  $T_{2g}(Q^1) + T_{1g}$  mode, as shown in Fig. 3, quantitatively accounts for the neutron intensities. The  $E_g + A_{1g}$  modes (not shown) cannot account for these data. Instead of the  $T_{2g}(Q^2)$  internal strain providing the mechanism for U-U coupling, the modes that dominate the cooperative Jahn-Teller effect are the oxygen internal shear deformations  $T_{2g}(Q^1) + T_{1g}$ . This linear combination of  $Q^1$  and  $T_{1g}$  rotation, rather than pure  $Q^1$ , does not affect the coupling between  $\Gamma_5$  states. Therefore, the dominance of the internal shear deformation is compatible with the essential features of Allen's theory that explain the first-order magnetic transition with no external distortion as well as other magnetic properties.

We have chosen a model (Fig. 3) in which propagation vectors of the shear deformation and magnetic structure are perpendicular. Such a model introduces anisotropy at the uranium site suggesting a noncollinear magnetic configuration. A calculation of the magnetic structure factors, including domain averaging, for this noncollinear model gives  $[\mu f(\vec{k})/\sqrt{2}]^2$  in Eq. (1), but the domain factor is increased from  $\frac{1}{3}$  to  $\frac{2}{3}$ . Thus, with a multidomain crystal, the collinear and noncollinear magnetic configurations produce identical neutron intensities. This four-sublattice magnetic structure may explain some of the unusual features of the infrared spectra,<sup>12</sup> and a reanalysis of the spin-wave spectra would definitely be required. The character of the oxygen-sublattice strain behavior (Fig. 3) suggests the need to measure the temperature dependence of the transverse acoustic phonons at the zone boundary, especially near  $T_N$ .

To summarize, we report the observation of an internal rearrangement of the oxygen sublattice below the ordering temperature in  $\text{UO}_2$ . The description of the effect requires a modification of the ideas proposed by Allen<sup>4</sup> and suggests a noncollinear spin configuration. The magnetoelastic energy is minimized by an *internal* rearrangement in such a way as to leave the dimensions of the overall unit cell unchanged. The consequence of our observation for other lanthanide<sup>13</sup> and actinide<sup>14</sup> systems is an important new step in the formulation of spin-lattice interactions.

We are grateful to M. H. Mueller for his interest throughout these investigations, R. L. Hitterman for experimental assistance, and S. K. Chan

for correspondence. It is a pleasure to thank S. J. Allen for pointing out the relevance of the four-sublattice spin structure.

\*Work supported by the U. S. Energy Research and Development Administration.

<sup>1</sup>B. C. Frazer, G. Shirane, D. E. Cox, and C. E. Olsen, Phys. Rev. **140**, A1449 (1965).

<sup>2</sup>R. A. Cowley and G. Dolling, Phys. Rev. **167**, 464 (1968).

<sup>3</sup>O. G. Brandt and C. T. Walker, Phys. Rev. **170**, 528 (1968).

<sup>4</sup>S. J. Allen, Phys. Rev. **166**, 530 (1968).

<sup>5</sup>S. J. Allen, Phys. Rev. **167**, 492 (1968).

<sup>6</sup>J. Faber, Jr., in *Magnetism and Magnetic Materials—1974*, edited by C. D. Graham, Jr., G. H. Lander, and J. J. Rhyne, AIP Conference Proceedings No. 24 (American Institute of Physics, New York, 1975), p. 51.

<sup>7</sup>D. F. Johnston, Proc. Phys. Soc., London **88**, 37 (1966); S. W. Lovesey and D. E. Rimmer, Rep. Prog. Phys. **32**, 333 (1969); G. H. Lander, T. O. Brun, and O. Vogt, Phys. Rev. B **7**, 1988 (1973).

<sup>8</sup>A. J. Freeman, J. P. Desclaux, G. H. Lander, and J. Faber, Jr., Phys. Rev. B (to be published).

<sup>9</sup>H. U. Rahman and W. A. Runciman, J. Phys. Chem. Solids **27**, 1833 (1966).

<sup>10</sup>D. S. Rodbell, unpublished. See also G. K. White and F. W. Sheard, J. Low Temp. Phys. **14**, 445 (1974), especially Ref. 31 and associated discussion. The results of J. D. Pirie and T. Smith [Phys. Status Solidi **41**, 221 (1970)] are consistent with our model, i.e., in which only the oxygen atoms move.

<sup>11</sup>J. Faber, Jr., and M. H. Mueller, to be published.

<sup>12</sup>S. J. Allen and P. J. Colwell, private communication.

<sup>13</sup>K. W. H. Stevens and E. Pytte, Solid State Commun. **13**, 101 (1973).

<sup>14</sup>G. H. Lander and M. H. Mueller, Phys. Rev. B **10**, 1994 (1974).

## Long-Range Migration of Self-Interstitial Atoms in Tungsten

F. Dausinger and H. Schultz

*Institut für Theoretische und Angewandte Physik der Universität Stuttgart, Stuttgart, Bundesrepublik Deutschland, and Institut für Physik im Max-Planck-Institut für*

*Metallforschung, Stuttgart, Bundesrepublik Deutschland*

(Received 18 August 1975)

Resistivity annealing following irradiation with 3-MeV electrons at 4.5 K has been investigated on tungsten single crystals. High-purity samples showed a recovery stage between 24 and 30 K, which apparently shifts with increasing dose to lower temperatures. We conclude that it is associated with long-range migration of self-interstitial atoms with a migration energy of  $54 \pm 5$  meV. The relationship to recent conclusions of other authors is discussed.

The long-range migration of self-interstitial atoms (SIA's) in tungsten at low temperatures has been the topic of two recent Letters. Okuda and Mizubayashi<sup>1</sup> presented results of internal-friction and dynamic-modulus measurements on single crystals following fast-neutron irradiation near 4.2 K. They suggest free migration of SIA's at  $\sim 15$  K and detrapping of SIA's from impurity atoms at  $\sim 30$  K. On the basis of field-ion microscope observations<sup>2-4</sup> Seidman, Wilson, and Nielsen<sup>2</sup> suggest free migration near 38 K.

Extending the work of Kunz *et al.*<sup>5</sup> we made a new approach to investigate the resistivity recovery in tungsten following 3-MeV electron irradiation at 4.5 K, varying the following three parameters: degree of purity, crystallographic orientation, and irradiation dose. The starting material of the high-purity samples had a residual-resistance ratio of  $\approx 70\,000$  (3.5 mm diam,

no size-effect correction). Experimental details are given elsewhere.<sup>6</sup>

Isochronal recovery stages which are connected with long-range migration are expected to be suppressed by impurities which trap the migrating SIA's. In Fig. 1, the four stages at 27, 43, 59, and 96 K are of this type, indicating long-range migration of SIA's at these temperatures. Further support for this supposition is given by the observation of Kunz *et al.*<sup>5</sup> that these stages are enhanced in prequenched samples.

One can expect further two types of recovery stages connected with long-range migration: (a) Stages shifting to lower temperatures with increasing Frenkel-defect concentration. Their reaction rate is determined by the random walk of the SIA's to vacancies (e.g., stage  $I_E$  in Cu). (b) Stages showing no dose shift. Their reaction rate is determined by the liberation of the SIA's